THE JOURNAL OF PHYSICAL CHEMISTRY B

Article

pubs.acs.org/JPCB

Manipulating Energy Transfer in Copolymer-Based Nanocomposites by Their Controlled Nanocaging and Release of an Ionic Styryl Dye: A Case of an Ultrasensitive pH Sensor

Anamika Manna, Dibakar Sahoo, and Sankar Chakravorti*

Department of Spectroscopy, Indian Association for the Cultivation of Science, Jadavpur, Kolkata 700032, India

ABSTRACT: We report an interesting pH-tunable energy transfer between an acceptor ionic styryl dye 2-(4-(dimethylamino)styryl)-1-methylpyridinium iodide and a donor charge-transfer dye 1,8-naphthalimide in a vesicular medium. The polyethylene-*b*-polyethylene glycol block copolymer intercalates with the sodium dodecyl sulfate anionic surfactant to form self-aggregated nanocomposites. These nanocomposites interact with the donor molecules in aqueous solution to form "vesicles", and the donor molecules become attached on the outer wall by hydrogen bonding. The acceptor molecules are observed to be loaded in the vesicular interior. By controlling the spectral overlap of the donor and acceptor molecules by changing the pH of the medium, the energy-transfer efficiency in vesicles has been studied. The efficiency of energy transfer in vesicular media (55%) is found to be less compared to that in aqueous media (80%) at pH 7. The fall in efficiency has been attributed to the perturbation imparted by the vesicular wall due to the good matching of the donor–acceptor distance with the wall thickness. At low pH, the efficiency shows an abrupt increase (95%) due to the release of the acceptor molecules from the vesicular medium causing subsequent reduction of donor–acceptor separation and an increase of the spectral overlap at that pH.

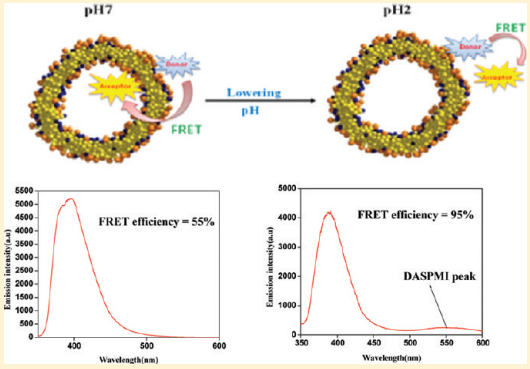

INTRODUCTION

The amphiphilic molecules that self-assemble to form biomimicking vesicles have proven to be efficient vehicles for drug delivery. Much work has been done recently to check its encapsulation ability for the hydrophobic drugs.[1−3] The amphiphilic copolymers are found to self-assemble into particular morphologies in dilute or semidilute solutions to form nanocomposites, and these polymeric vesicles are very useful as delivery vectors.[4−7] The nanoassemblies formed by the polymers containing PEG chains are particularly more important biologically due to their greater stability and low critical micellar concentration. These nanocomposites can also solubilize the drugs into the living cells, which are basically insoluble in water, which makes these systems more interesting to be used as detectors. The stimuli-responsive systems have attracted much interest in recent years due to their broad usage in targeted drug delivery and molecular sensors. In particular, the molecular sensors comprised of such biomimetic nanocomposites are capable of detecting the environmental changes in living cells and have potential applications in biotechnology. Fluorescence resonance energy transfer (FRET) is nonradiative energy transfer from excited-state donors to the ground-state acceptors, which has been applied extensively in medical and biological applications in studying the environment around the living cells at the molecular level.[8−10] With the FRET efficiency being highly dependent on the distance between the donor and the acceptor, a drastic change in efficiency of the FRET in response to a particular stimulus makes it very useful as a stimuli-responsive molecular sensor. The broad use of the biomimicking polymeric nanocomposites in different biomedical applications makes these systems very interesting to be studied as FRET probes to detect the environment around living cells. Conjugated polymers showing the FRET mechanism have attracted much attention.[11] By a fast electrostatic mechanism, ionic styryl dyes like 2-(4-(dimethylamino)styryl)-1-methylpyridinium iodide (DASPMI) (Scheme 1a) are known to respond to changes in the transmembrane potential.[12−14] This makes DASPMI a valuable tool to measure the membrane potential of mitochondria[15,16] in living cells. The cationic dye DASPMI shows an interesting multibond rotation involved intramolecular charge-transfer (ICT) photophysical property.[17,18] The strong dependence of its photophysics on the viscosity and polarity of the medium also makes this dye useful in polymer science and in cell biology.[19−21]

1,8-Naphthalimide (NAPMD) undergoes ICT in nonpolar media. In polar solvents, NAPMD undergoes intermolecular proton transfer,[22] thus forming anionic NAPMD (Scheme 1b). The ICT state of NAPMD is highly sensitive to its microenvironment. The high sensitivity of these two dyes toward their environment proves them to be very useful environmentally sensitive FRET pairs. The block copolymers self-assemble in aqueous solution to form spherical structures, as studied

Received: December 7, 2011
Revised: January 31, 2012
Published: February 6, 2012

Scheme 1. (a) Mechanism of ICT in DASPMI at pH 7 and at Low pH Values and (b) Mechanism of Formation of the Anionic NAPMD in the Aqueous Solution (Protic Solvent)

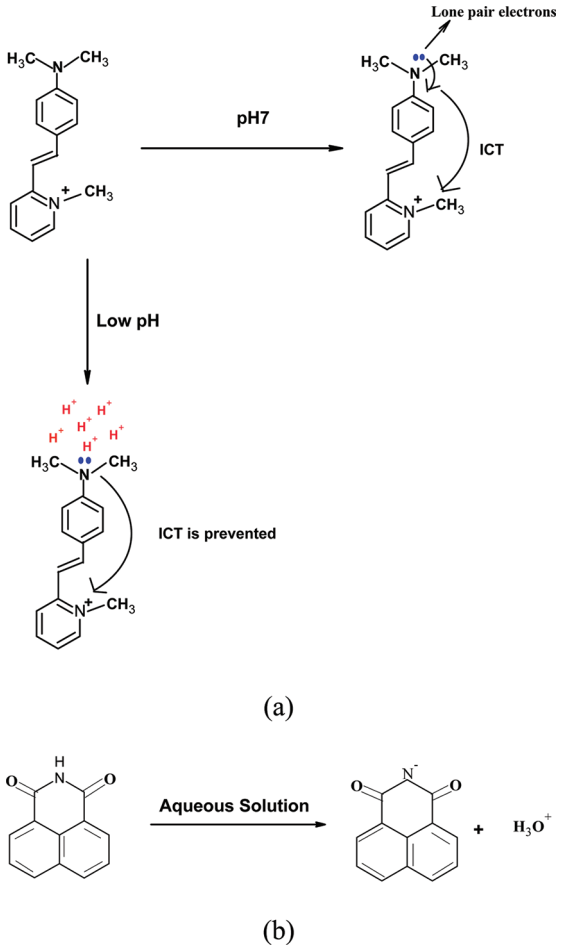

theoretically by Srinivas et. al using coarse-grain dynamics.[23] In an earlier communication, it was established that the block copolymer polyethylene-*b*-polyethylene glycol (PE-*b*-PEG), upon interaction with an anionic surfactant sodium dodecyl sulfate (SDS), forms a water-tight microenvironment[24] due to the entanglement of the block copolymer with the surfactant chains. In this work, we envisaged to explore the energy transfer between the DASPMI (acceptor) and the NAPMD (donor) molecules in this water-tight nanocomposite. Upon addition of NAPMD to the above-mentioned block copolymer−micelle nanocomposite in aqueous solution, some vesicle-like structures were observed to form with NAPMD molecules attached to the wall of these vesicles. Therefore, the problem boiled down to FRET between vesicles containing donor NAPMD and acceptor DASPMI molecules. The vesicles formed by PEG lipids were found to result in an extended circulation time, carrying anticancerous drugs to find their way to hidden tumors. The chains of PEG are also notable for imparting biocompatibility to membranes.[25] Therefore, the vesicles formed from the block copolymer of the PEG polymer (i.e., PE-*b*-PEG) seem to be an interesting medium for studying the FRET. In this paper, we report a study of the efficiency of energy transfer in the vesicle system and its modulation with pH variation versus that in aqueous medium. The pH detection by FRET was especially very important as it could be applied for optical detection of tumor cells that have a lower pH around their environment.[26,27]

EXPERIMENTAL DETAILS

The compounds NAPMD and DASPMI were procured from Aldrich Chemical Co. and were recrystallized before use. SDS and PE-*b*-PEG ($M_w \approx 575$, $m \approx 57$, $n \approx 60$) were used as received from Fluka or Aldrich Chemicals, U.S.A. Deionized water (Millipore) was used for measurement of absorption and fluorescence spectra. PE-*b*-PEG, 1 mg/mL (a concentration much higher than the CMC of PE-*b*-PEG), was added to an aqueous solution of 25 mM SDS micelle, which forms a nanocomposite. The absorption spectra were taken with a Shimadzu UV−vis absorption spectrophotometer (model UV-2401PC). A Hitachi F-4500 fluorescence spectrophotometer was used to obtain the steady-state emission spectra. For the spectroscopic measurements, the sample concentration was maintained at 10^{-5} M in each case in order to avoid aggregation, and emission was corrected for all optical components. For the measurement of the pH of the solutions used in the experiment, a digital pH meter (model DPH 504 of Global electronics) was used. The pH of the vesicular medium was adjusted by adding almost 5−20 μL of HCl aqueous solution (0.1, 0.01, or 0.001 M) into the sample suspensions (3 mL), and it was measured with the pH meter. The slight concentration changes ($0-2 \times 10^{-7}$ M) were negligible. All experiments were done at room temperature.

Field emission scanning electron microscopy (FESEM) (JSM-6700F, from JEOL, Japan) was used to record the scanning electron micrograph images of PE-*b*-PEG and SDS micellar aggregates.

A transmission electron microscope (JEOL, JEM-2010, Japan) operated at 200 KV was employed to take the TEM images. For the observation of the vesicles, a drop of sample suspension (0.5 mg mL^{-1}) was placed on 200-mesh Formvar copper grids coated with carbon. About 2 min after the deposition, the grid was tapped with filter paper to remove surface water. After 1 min, the surface water on the grid was removed by tapping with filter paper.

For SEM measurements, the sample films were prepared and dried overnight, and for TEM, the sample films were taken on copper grids and dried overnight.

RESULTS AND DISCUSSION

We already know that NAPMD undergoes intermolecular charge transfer[22] in aqueous solution, thus forming anionic NAPMD. The fluorescence band of anionic NAPMD is obtained at 395 nm (when excited at 340 nm). The anionic NAPMD fluorescence band is observed to be highly sensitive toward changing pH. The anionic NAPMD fluorescence band quenches as the pH is lowered. The block copolymer (PE-*b*-PEG) interacts with the anionic surfactant (SDS) by ion−dipole interaction, and they intercalate with each other to form spherically aggregated nanostructures in the aqueous solution.[28,29]

Formation of these spherical nanocomposites was confirmed by SEM images in our early study.[24] In aqueous solution, we studied the interaction of NAPMD with this nanocomposite. We observed that the fluorescence band of anionic NAPMD shows quenching along with a slight blue shift of 2 nm upon interaction with the nanocomposites (complex of SDS and the nonionic block copolymer) above the CAC (critical aggregation concentration) of the mixture. The quenching in the anionic band of NAPMD is due to the hydrogen bonding of the anionic NAPMD with the PEG group on the outer wall of this nanocomposites.[30] The TEM images of these nanocomposites

dx.doi.org/10.1021/jp211776m | J. Phys. Chem. B 2012, 116, 2464−2471

probed with NAPMD show formation of some vesicle-like structures with thick dark outer walls (Figure 1a), which are

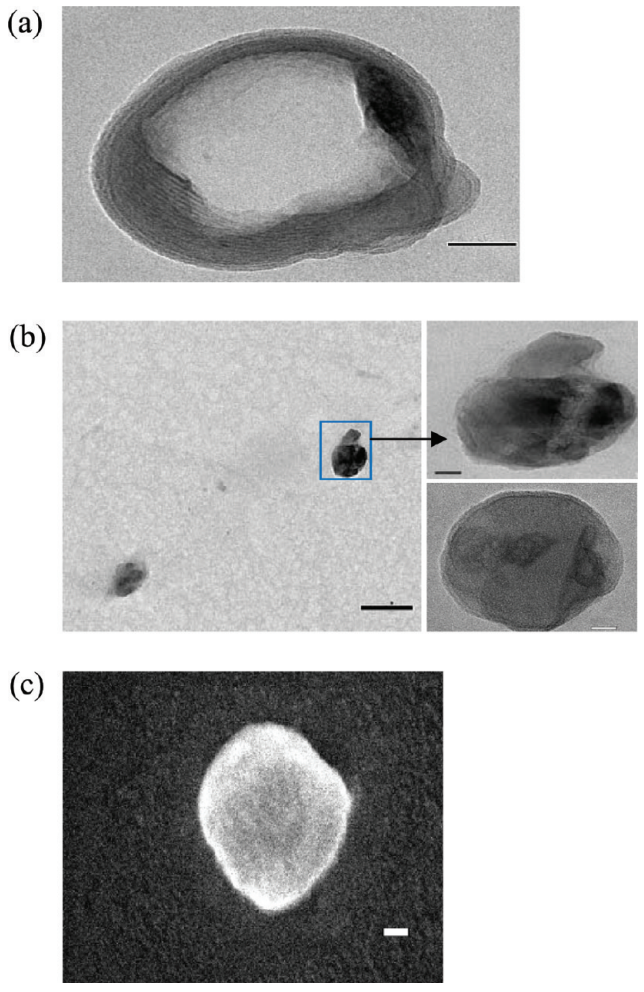

Figure 1. TEM image of (a) unloaded vesicle formed due to the interaction of the NAPMD (5×10^{-5} M) with the diblock copolymer–SDS nanocomposite (scale bar = 50 nm) and (b) vesicles with DASPMI loaded at the core showing a dark interior (scale bar = 20 nm) and (c) the SEM image of the spherically shaped vesicles with DASPMI molecules loaded inside of the core (scale bar = 100 nm).

detected as "multilamellar vesicles".[31] Previously, we reported the formation of these vesicles and studied the effect of pH on these vesicles.[32] These structures are quite different from the copolymer–SDS nanocomposite structures as observed in our previous study.[24] This phase transformation may arise due to the alteration of the hydrophilic/hydrophobic ratio of the PE-*b*-PEG polymer as caused by interaction with anionic NAPMD.[23] The anionic NAPMD molecules interact with the PEG group on the outer wall of the nanocomposite by hydrogen bonding and prefer to reside on the vesicular wall, as evinced by the blue shift in fluorescence studies as well.

The ionic styryl dye DASPMI shows an absorption band maximum at 435 nm and the fluorescence band maximum at 570 nm. The band at 570 nm arises due to the ICT state of DASPMI in the excited state.[33] DASPMI is a cationic dye. In the excited state, DASPMI undergoes ICT, which in turn reduces the cationic form of DASPMI in the aqueous solution (Scheme 1a). The absorption band of DASPMI is seen to remain unaffected with changing pH.

The TEM images of the vesicles after the addition of DASPMI show a dark interior (Figure 1b), as corroborated by SEM images as well (Figure 1c). Comparing the TEM image prior to addition of DASPMI (unloaded vesicles), the TEM observations show that the acceptor molecules (DASPMI) are loaded inside of the interior of the vesicles. The gray vesicular wall is clearly distinguishable from the dark corona containing the DASPMI molecules, unlike the unloaded vesicles (Figure 1a). According to the electron microscopic results, we find the diameter and wall thickness of the empty vesicles to be 300 and 40 nm, respectively, as opposed to the acceptor loaded vesicles, which have a diameter and wall thickness of 127 and 6 nm, respectively. Inclusion of the DASPMI molecules in the core of the vesicles reduces the curvature of the vesicles, thus resulting in shrinkage of the vesicular size.

NAPMD and DASPMI make an ideal FRET pair because of nice overlap of the fluorescence band of anionic NAPMD and the absorption band of DASPMI in an aqueous medium, and also, the absorption bands of the donor (340 nm) and the acceptor (435 nm) are well separated. Thus, these donors and acceptors can be selectively photoexcited in aqueous media without mutual interference.

The FRET efficiency of the donor–acceptor conjugate depends on the (i) distance, (ii) orientation factor, (iii) and overlap integral of the donor and the acceptor. The donor–acceptor distance can effectively be controlled for the energy transfer in the vesicles by changing the pH of the medium because the donor fluorescence is highly sensitive to pH. The anionic NAPMD fluorescence band (at 393 nm) in the vesicle medium is found to overlap partially with the DASPMI absorption band (at 435 nm). From the overlap of the bands, it seems that the anionic NAPMD attached to the vesicle wall can serve as an efficient donor and the cationic DASPMI molecules can serve as the acceptor for a preferential energy transfer between them. As DASPMI is gradually added to the vesicular system containing anionic NAPMD on the wall, the fluorescence intensity of anionic NAPMD in the vesicles (at 393 nm) gradually quenches (when excited at 340 nm) with increasing concentration of DASPMI (Figure 2), showing a preferential

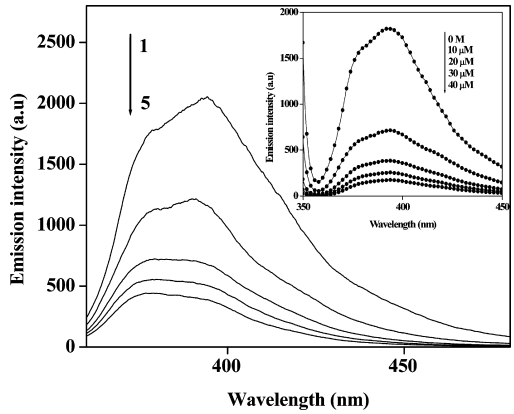

Figure 2. Fluorescence spectra of 5×10^{-5} M anionic NAPMD (when excited at 340 nm) in vesicular media with increasing concentration of DASPMI, (1) 0, (2) 10, (3) 20, (4) 30, and (5) 40 μM. (Inset) Fluorescence spectra of 5×10^{-5} M anionic NAPMD (excited at 340 nm) at pH 2 attached to the vesicle wall with increasing concentration of DASPMI, 0–40 μM.

energy transfer between the FRET pair. The fluorescence band of DASPMI (at 570 nm) could not be observed in the energy-transfer process due to its lower quantum yield value (0.03) compared to that of NAPMD (0.6) in aqueous media.

dx.doi.org/10.1021/jp211776m | *J. Phys. Chem. B* 2012, 116, 2464–2471

The energy transfer between the two dyes is quantified using the following equations[34,35]

$$J = \frac{\int_{\infty}^{0} F_D(\lambda)\varepsilon_A(\lambda)\lambda^4 \, d\lambda}{\int_{\infty}^{0} F_D(\lambda) \, d\lambda} \quad (1)$$

$$R_0 = 0.211[K^2\eta^{-4}\varphi_D J(\lambda)]^{1/6} \quad (2)$$

$$E = \frac{nR_0^6}{nR_0^6 + r_{DA}^6} \quad (3)$$

where λ is the wavelength, ε_A is the extinction coefficient of the acceptor, R_0 is the Förster distance at which the energy-transfer efficiency is 50%, k^2 is the orientation factor, η is the refractive index of the medium, Φ_D is the fluorescence quantum yield of donors in the absence of acceptors, r_{DA} is the donor-to-acceptor distance, and n is the molar ratio of acceptors to donors.

The FRET efficiency (E) for the acceptor-loaded vesicles is found to be ~0.55 as calculated from eq 3. The overlap integral (J) at pH 7 is calculated to be 162.6 × 10^{13} M^{-1} cm^{-1} nm^4, and the distance between the donor and acceptor is found to be ~6.4 nm. The energy transfer is studied in aqueous media as well in the absence of the vesicles. The fluorescence band of anionic NAPMD in aqueous solution (at 395 nm) quenches (when excited at 340 nm) with gradual addition of DASPMI (Figure 3). The fluorescence band of DASPMI (at 570 nm) is

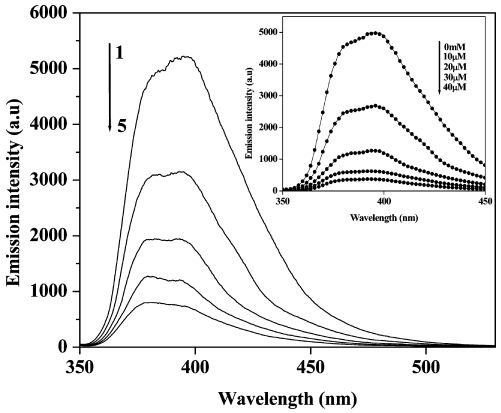

Figure 3. Fluorescence spectra of 5 × 10^{-5} M anionic NAPMD (excited at 340 nm) obtained in the aqueous solution with increasing concentration of the DASPMI, (1) 0, (2) 10, (3) 20, (4) 30, and (5) 40 μM. (Inset) Fluorescence spectra of anionic NAPMD (excited at 340 nm) at pH 2 in aqueous solution with increasing concentration of DASPMI.

suppressed in this energy-transfer process, similar to the reason cited earlier in vesicular media. The FRET efficiency in aqueous media is equal to 0.8, as evaluated from eq 3. The FRET efficiency is strong enough when the donor and the acceptor are in close proximity, that is, they are closer than the Förster's radius (R_0). This higher FRET efficiency in aqueous media may be attributed to strong electrostatic interaction between the oppositely charged FRET pair and the decreased donor–acceptor distance. Taking a cue from the above inferred mechanism of electrostatic interaction in the energy transfer between the donor and the acceptor molecules in aqueous media, it may be assumed that the same mechanism is true for the energy transfer between the acceptor-loaded vesicles and the donors attached to the wall of the vesicle. In vesicles, the efficiency of the energy transfer may be reduced due to the increased donor-to-acceptor distance arising out of the perturbation due to the intervening wall of the amphiphilic vesicle (containing block copolymer and surfactant) between the FRET pair causing a consequent decrease in electrostatic interactions between the donor and acceptor molecules. In the present case, the vesicle wall thickness of about 6 nm, measured from the TEM image, matches well with the donor–acceptor distance (calculated FRET distance $r \approx 6.4$ nm) for energy transfer in the vesicles at pH 7, which supports the above-mentioned proposition of attachment of NAPMD on the wall of the vesicles and the DASPMI in the interior. This increased FRET distance (compared to an r value of ~5 nm in water) in the vesicle system reduces the FRET efficiency (0.55) between the pair in the vesicles.

The pH-dependent donor fluorescence spectra controls the overlap integral (J), which is highly related to the energy-transfer efficiency between the FRET pair. As the pH of the solution is lowered, the overlap integral increases, and the efficiency of energy transfer (E) also increases abruptly (inset of Figure 2). Thus, the efficiency of energy transfer depends highly on the pH of the medium. The anionic NAPMD fluorescence band quenches as the pH is lowered, and consequently, a blue-shifted fluorescence band of the DASPMI (at 550 nm) gradually reappears (Figure 4)

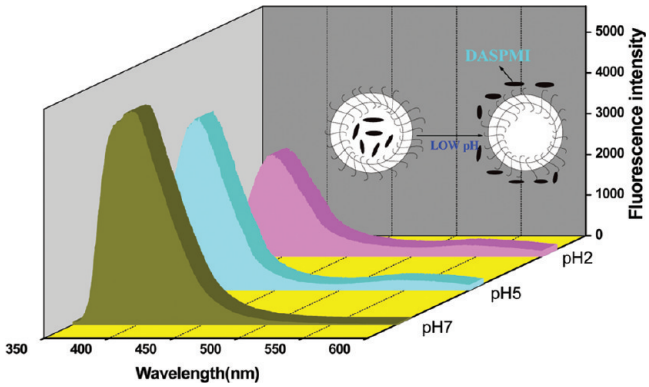

Figure 4. Gradual rise of the low-energy fluorescence band of DASPMI molecules along with the high-energy fluorescence band of anionic NAPMD (when excited at 340 nm) obtained in vesicles when the pH is lowered from pH = 7 to 2, causing easy release of DASPMI molecules from the vesicle interior at lower pH, thus enhancing the FRET efficiency.

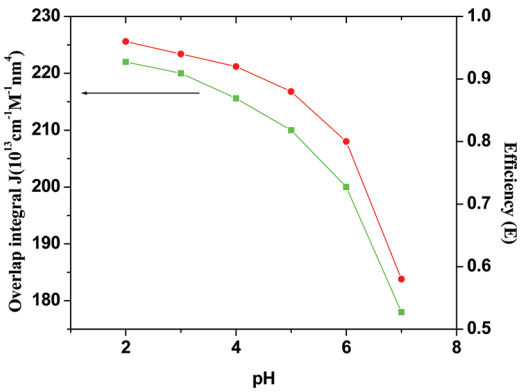

Figure 5. The pH dependence of the energy-transfer efficiency (red line) and overlap integral (green line) as the pH is decreased from pH = 7 to 2.

(when excited at 340 nm). At pH 7, the DASPMI fluorescence is not detectable due to its low quantum yield value, whereas upon

dx.doi.org/10.1021/jp211776m | J. Phys. Chem. B 2012, 116, 2464–2471

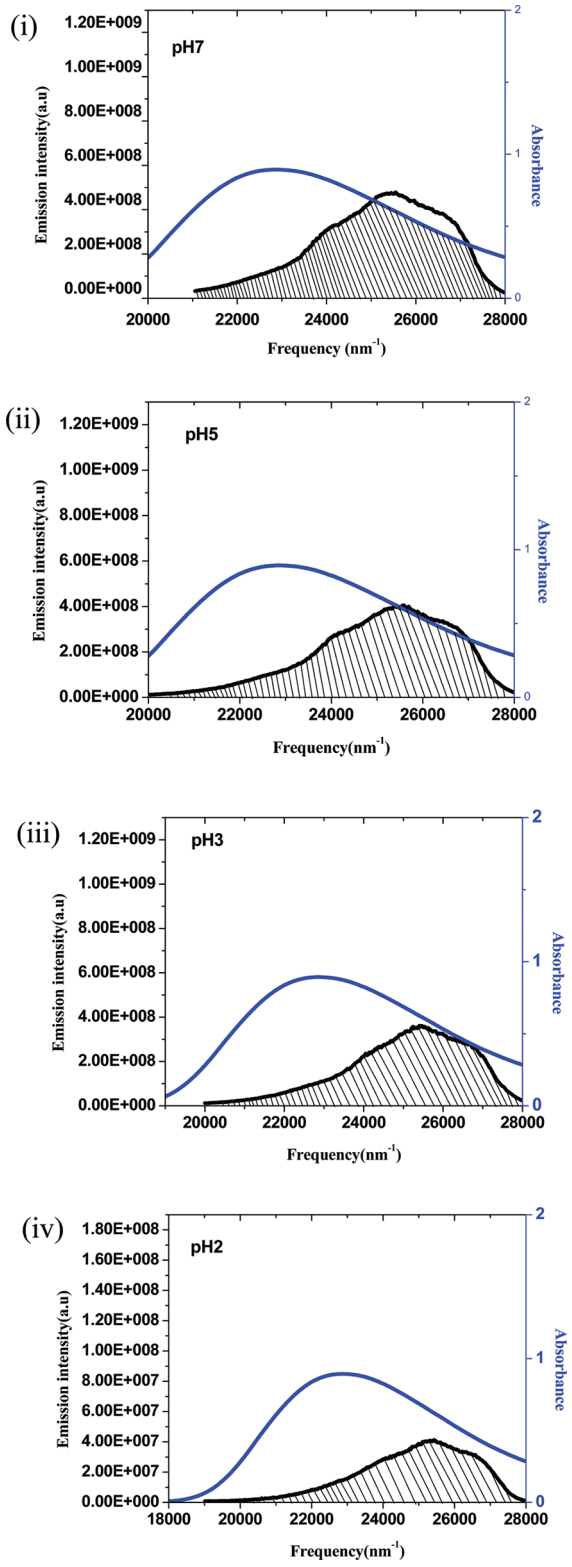

Figure 6. Spectral overlap of the fluorescence band of NAPMD anions (Black outline) and the absorbance of DASPMI (blue outline) when excited at 340 nm at pH (i) 7, (ii) 5, (iii) 3, and (iv) 2 for [NAPMD] = 5×10^{-5} M and [DASPMI] = 4×10^{-5} M.

lowering the pH, the DASPMI fluorescence band reappears, which proves that the energy transfer increases highly at lower pH, leading to enhanced DASPMI (acceptor) fluorescence intensity. At pH 5, the efficiency is $E \approx 0.88$, the J value is calculated to be 200×10^{13} M^{-1} cm^{-1} nm^4, and the donor-to-acceptor distance is ~5.2 nm. Thus, with decreasing pH, the E and J values increase (Figure 5), and consequently, the donor-to-acceptor distance decreases, thereby enhancing the energy transfer between the anionic NAPMD attached to the vesicular wall and the DASPMI molecules in the interior of the vesicles. As indicated by the overlap graphs (the overlap regions are indicated by the shaded regions), the overlap between the donor fluorescence and the acceptor absorption increases preferably with decreasing pH (Figure 6). There is a complete overlap at pH 2, and the efficiency is also at a maximum at ~0.95.

The TEM image of the acceptor-loaded vesicles after lowering the pH shows an interesting result; the vesicles are observed with a vacant interior with the same size and wall thickness as that of the unloaded vesicles (Figure 7). Thus, the

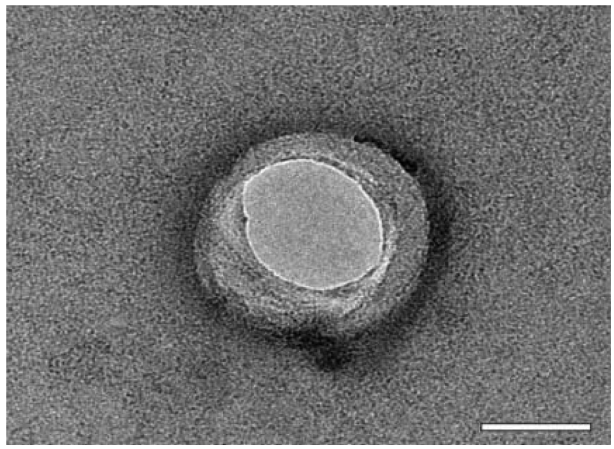

Figure 7. TEM image of the unloaded amphiphilic vesicle as obtained at pH 2 (scale bar = 100 nm).

TEM observations reveal that at low pH, the DASPMI molecules are released from the interior of the vesicles, returning the vesicles back to the normal shape and size, similar to that of the unloaded vesicles. As a control experiment, the energy-transfer efficiency is observed to increase highly upon lowering the pH of the aqueous medium (inset of Figure 3). At pH 2, the efficiency is found to be $E \approx 0.98$. The value of E at pH 2 is evaluated to be much higher compared to that at pH 7.

At pH 7, the DASPMI fluorescence band is suppressed in the energy-transfer process. As the pH is lowered, the fluorescence band for DASPMI is observed to reappear (when excited at the donor excitation wavelength) with a blue shift of 20 nm, similar to that in vesicles, thus showing an efficient energy transfer between the FRET pair. To explain the above blue shift of DASPMI at low pH, the effect of low pH has been studied on the fluorescence band of DASPMI in aqueous media. The fluorescence band of DASPMI is observed to be blue-shifted by 20 nm with the lowering of pH. This blue shift in the fluorescence ICT band of DASPMI indicates the destabilization of the ICT state of DASPMI at lower pH. DASPMI in the excited state undergoes ICT, thus reducing the cationic part of DASPMI in the excited state. The excess protons in the low-pH media prevent this charge transfer in the DASPMI in the excited state, resulting in an enhanced cationic form of DASPMI (Scheme 1a). Thus, the lowered pH destabilizes the ICT state in DASPMI in the excited state, which is reflected by the blue shift in the fluorescence band of DASPMI as well.

dx.doi.org/10.1021/jp211776m | J. Phys. Chem. B 2012, 116, 2464–2471

Scheme 2. Schematic Representation of the Energy Transfer between the DASPMI Molecules Loaded in the Core of the Vesicles and the NAPMD Anions Attached to the Vesicular Wall at pH 7 and at Lower pH, Showing Increased Interaction (as the DASPMI molecules are released from the vesicle interior) at Lower pH, Giving a Blue-Shifted Emission Band of DASPMI

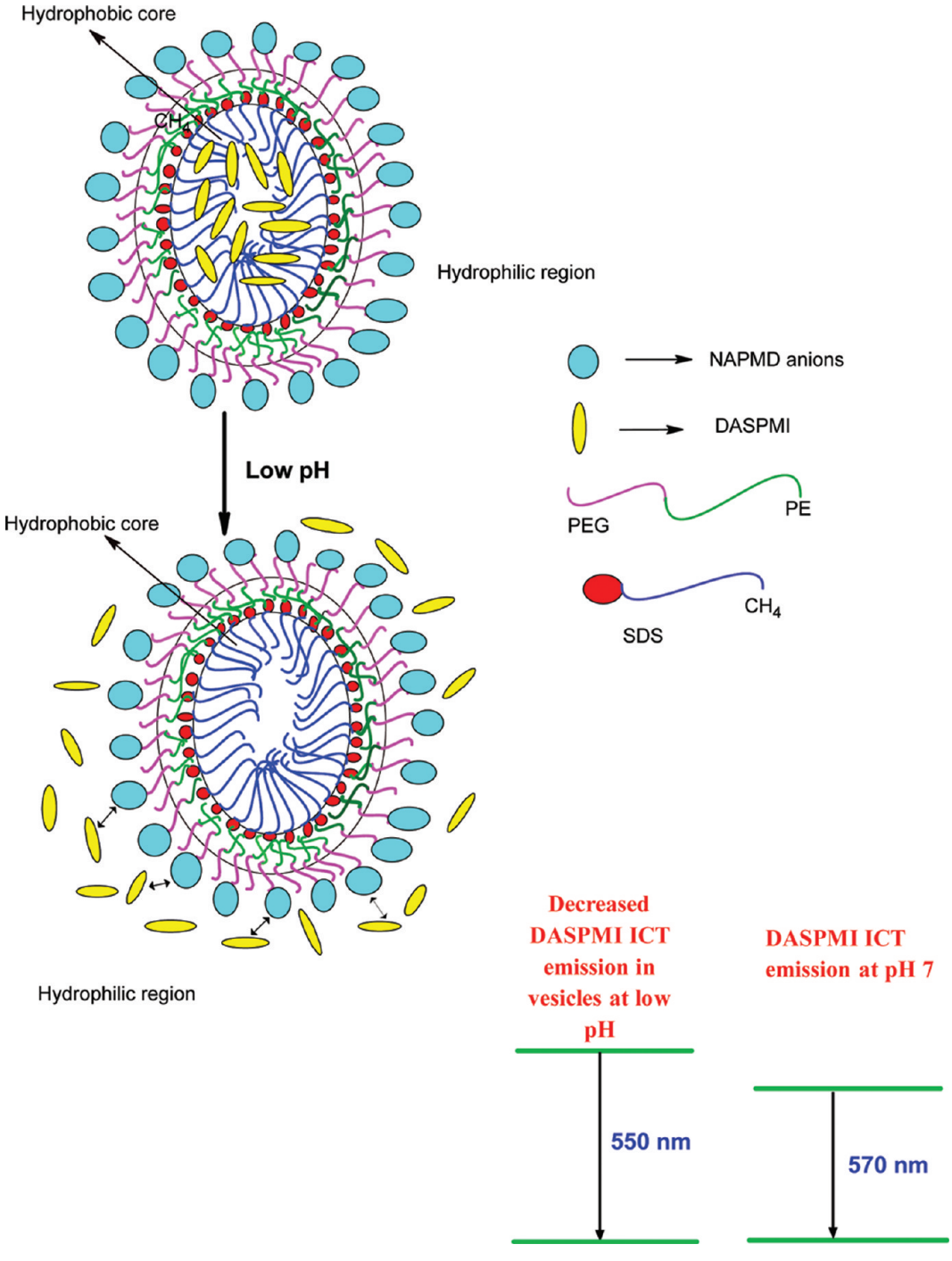

This enhanced cationic form of DASPMI causes an increased electrostatic interaction with the anionic NAPMD molecules in aqueous media, causing a further decrease of the donor-to-acceptor distance and consequently an efficient energy transfer between the donor and the acceptor molecules at low pH. For the energy transfer in the vesicular system at lower pH values, DASPMI is released from the interior of the vesicles, as revealed by the TEM images, and at the same time, the cationic form of DASPMI is also enhanced due to destabilization of the ICT state of DASPMI (Scheme 2). The FRET efficiency in aqueous media at low pH (0.98) is observed to match quite well with the efficiency value in vesicles at low pH (0.95). This proves the fact that at low pH, the acceptor molecules are released from the interior of the vesicles and give a similar enhanced efficiency as that in aqueous solution due to enhancement of the electrostatic interaction between the FRET pair. It is now clear that the energy-transfer efficiency between the acceptor-loaded vesicles and the donor molecules attached to the vesicular wall decreases abruptly with lowering of the pH value of the

dx.doi.org/10.1021/jp211776m | J. Phys. Chem. B 2012, 116, 2464−2471

medium, causing an enhanced energy transfer between the FRET pair (Figure 8).

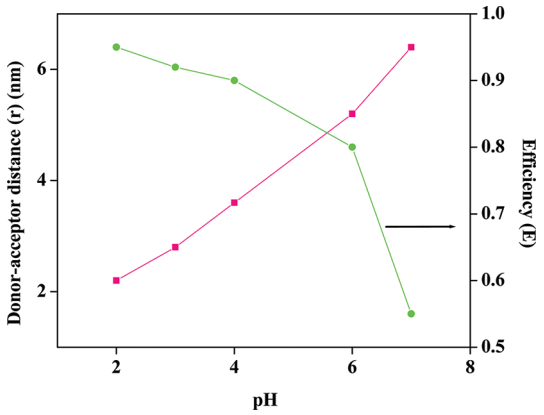

Figure 8. The dependence of energy-transfer efficiency (green line) and donor–acceptor distance (pink line) with decreasing pH of the solution from pH = 7 to 2.

TIME RESOLVED FLUORESCENCE SPECTROSCOPY

To elucidate the energy transfer properly, the decay times of both the donor and the acceptor molecules were recorded and compared in the vesicular medium at pH = 7 and 2. We know that the decay time of NAPMD in aqueous solution was fitted monoexponentially with a time constant of 2.5 ns ($a_1 \approx 100$),[24] and the decay time of DASPMI in the aqueous solution was fitted biexponentially with time constants of 0.6 ($a_1 \approx 70$) and 1.4 ns ($a_2 \approx 30$) for the LE and ICT states, respectively.[33] In vesicular media, the decay time of NAPMD anions was found to decrease to 2.1 ns due to the binding of the NAPMD anions to the vesicular wall, and the lifetime of DASPMI increased to 0.9 ($a_1 \approx 15$) and 2.02 ns ($a_2 \approx 83$) due to the inclusion of the DASPMI molecules in the interior of the vesicle core. At pH 2, the lifetime of NAPMD in vesicular media further decreased to 1.9 ns ($a_1 \approx 98$), and for DASPMI, the decay times were obtained to be 0.7 ($a_1 \approx 11$) and 3.65 ns ($a_2 \approx 89$), and a rise time of ~1 ns for the acceptor was obtained. At low pH, the acceptor rise time in vesicles almost followed the donor decay time, thus showing a favorable energy transfer.

CONCLUSION

We report here the pH-controlled energy-transfer mechanism in vesicles manipulated by the pH-sensitive nanocaging and release of acceptor DASPMI molecules from the interior of the vesicles, which can act as a smart pH sensor of the medium. Anionic NAPMD interacts with the nanocomposite of the diblock copolymer and anionic micelle, forms multilamellar vesicles, and is attached to the outer wall by hydrogen bonding. The interaction at pH 7 between the acceptor cationic DASPMI molecules loaded in the interior of the vesicles and the donor anionic NAPMD molecules on the wall is perturbed by the vesicular wall, thus giving a lowered FRET efficiency ~55%. The fascinating feature of these loaded vesicles is that as the pH is lowered, the DASPMI molecules are released from the interior of the vesicles, which in turn decreases the donor–acceptor distance, giving an enhanced FRET efficiency ~95%. Normally, the environment around the tumor cells is found to have a lower pH. Thus, the abrupt increase of the energy-transfer efficiency at low pH in these PEG-based vesicles can act as a good photodetector to detect the tumor cells efficiently. It is known that the photons in the 240–340 nm range can destroy the living cells. In our work, we have excited at the exact absorption peak of NAPMD (340 nm), but if we look at the absorption band of NAPMD, we can get a similar set of results by just shifting the excitation wavelength a little bit by 5–10 nm to avoid any physiological damage.

AUTHOR INFORMATION

Corresponding Author

*E-mail: spsc@iacs.res.in. Phone: +91-33-24734971 (Ext. 250). Fax: +91-33-2473-2805.

Notes

The authors declare no competing financial interest.

REFERENCES

(1) Soussan, E.; Cassel, S.; Blanzat, M.; Rico-Lattes, I. *Angew. Chem., Int. Ed.* **2009**, *48*, 274–288.
(2) Kataoka, K.; Harada, A.; Nagasaki, Y. *Adv. Drug Delivery Rev.* **2001**, *47*, 113–131.
(3) Ganta, S.; Devalapally, H.; Shahiwala, A.; Amiji, M. *J. Controlled Release* **2008**, *126*, 187–204.
(4) Ghoroghchian, P. P.; Frail, P. R.; Susumu, K.; Blessington, D.; Brannan, A. K.; Bates, F. S.; Chance, B.; Hammer, D. A.; Therein, M. J. *Proc. Natl. Acad. Sci. U.S.A.* **2005**, *102*, 2922.
(5) Photos, P. J.; Bacakova, L.; Discher, B.; Bates, F. S.; Discher, D. E. *J. Controlled Release* **2003**, *90*, 323.
(6) Ahmed, F.; Pakunlu, R. I.; Srinivas, G.; Brannan, A.; Bates, F.; Klein, M. L.; Minko, T.; Discher, D. E. *Mol. Pharmacol.* **2006**, *3*, 340.
(7) Broz, P.; Benito, S. M.; Saw, C.; Burger, P.; Heider, H.; Pfisterer, M.; Marsch, S.; Meier, W.; Hunziker, P. *J. Controlled Release* **2005**, *102*, 475.
(8) Lakowicz, J. R. *Principles of Fluorescence Spectroscopy*; Kluwer Academic/Plenum Publishers: New York, 1999.
(9) van der Meer, B. W.; Cocker, G., III; Simon Chen, S.-Y. *Resonance Energy Transfer, Theory and Data*; VCH: New York, 1994.
(10) Sahoo, D.; Bhattacharya, P.; Chakravorti, S. *J. Phys. Chem. B* **2010**, *114* (32), 10442–10450.
(11) McQuade, D. T.; Pullen, A. E.; Swager, T. M. *Chem. Rev.* **2000**, *100*, 2537.
(12) Loew, L. M.; Bonneville, G. W.; Surow, J. *Biochemistry* **1978**, *17*, 4065.
(13) Loew, L. M.; Scully, S.; Simpson, L.; Waggoner, A. S. *Nature* **1979**, *281*, 497.
(14) Loew, L. M.; Simpson, L. L. *Biophys. J.* **1981**, *34*, 353.
(15) Bereiter-Hahn. *J. Biochim. Biophys. Acta* **1976**, *423*, 1.
(16) Bereiter-Hahn, J.; Seipel, K. H.; Vöth, M.; Ploem, J. S. *Cell Biochem. Funct.* **1983**, *1*, 147.
(17) Strehmel, B.; Seifert, H.; Rettig, W. *J. Phys. Chem. B* **1997**, *101*, 2232.
(18) Strehmel, B.; Rettig, W. *J. Biomed. Opt.* **1996**, *1*, 98.
(19) Spooner, S. P.; Whitten, D. G. In *Photochemistry in Organized & Constrained Media*; Ramamurthy, V., Ed.; Wiley-VCH: Weinheim, Germany, 1991; pp 691–739.
(20) Ulmann, A. *An Introduction to Ultrathin Organic Films: From Langmuir–Blodgett to Self-Assembly*; Academic Press: San Diego, CA, 1991; Chapters 3 and 5.
(21) Ephardt, H.; Fromherz, P. *J. Phys. Chem.* **1991**, *95*, 6792.
(22) Manna, A.; Chakravorti, S. *Photochem. Photobiol.* **2010**, *86*, 47–54.
(23) Srinivas, G.; Discher, D. E.; Klein, M. L. *Nat. Mater.* **2004**, *3*, 638–644.
(24) Sahoo, D.; Bhattacharya, P.; Chakravorti, S. *J. Phys. Chem. B* **2009**, *113*, 13560–13565.
(25) (a) Harris, J. M., Zalipsky, S., Eds., *Poly(ethylene glycol):Chemistry and Biological Applications*; American Chemical Society: Washington, DC, 1997. (b) Also, as reviewed in: *Liposomes in Gene Delivery*; Lasic, D., Ed; CRC Press, Inc.: Boca Raton, FL, 1997; Chapter 10. PEG chain

lengths that optimize the stealth of liposomes, that is, lipid-conjugated PEG leading to the longest blood circulation time of liposomes, are in the approximate range of EO34 to EO114.
(26) Vaupel, P.; Kallinowski, F.; Okunieff, P. *Cancer Res.* **1989**, *49*, 6449−6465.
(27) Wike-Hooley, J. L.; Haveman, J.; Reinhold, H. S. *Radiother. Oncol.* **1984**, *2*, 343−366.
(28) Dai, S.; Tam, K. C. *J. Phys. Chem. B* **2001**, *105*, 10189.
(29) Zhang, G.; Chen, X.; Xie, Y.; Zhao, Y.; Qiu, H. *J. Colloid Interface Sci.* **2007**, *315*, 601.
(30) Noto, V. D.; Longo, D.; Mu1nchow, V. *J. Phys. Chem. B* **1999**, *103*, 2636−2646.
(31) Oyaizu, K.; Shiba, Y.; Nakamura, Y.; Yuasa, M. *Langmuir* **2006**, *22* (12), 5261−5265.
(32) Manna, A.; Chakravorti, S. *Photochem. Photobiol.* **2012**, DOI: 10.1111/j.1751-1097.2011.01049.x.
(33) Ramadass, R.; Bereiter-Hahn, J. *J. Phys. Chem. B* **2007**, *111*, 7681−7690.
(34) Lakowicz, J. R. *Principles of Fluorescence Spectroscopy*; Plenum: New York, 1999.
(35) Medintz, I. L.; Uyeda, H. T.; Goldman, E. R.; Mattoussi, H. *Nat. Mater.* **2005**, *4*, 435−446.